WAAS-Based Flight Inspection System

Euiho Kim, Todd Walter, and J. David Powell, *Stanford University*

BIOGRAPHY

Euiho Kim is a Ph.D. candidate in the Aeronautics and Astronautics Department at Stanford University. He received his B.S. in Aerospace Engineering in 2001 from Iowa State University and his M.S. from Stanford University in 2002. His research currently focuses on precise positioning using GPS/WAAS and flight inspection systems.

Dr. Todd Walter received his B. S. in physics from Rensselaer Polytechnic Institute and his Ph.D. in 1993 from Stanford University. He is currently a Senior Research Engineer at Stanford University. He is a co-chair of the WAAS Integrity Performance Panel (WIPP) focused on the implementation of WAAS and the development of its later stages. Key contributions include: early prototype development proving the feasibility of WAAS, significant contribution to MOPS design and validation, co-editing of the Institute of Navigation's book of papers about WAAS and its European and Japanese counterparts, and design of ionospheric algorithms for WAAS. He was the co-recipient of the 2001 ION early achievement award.

Prof. J. David Powell received his B.S. degree in Mechanical Engineering from MIT and his Ph.D in Aero/Astro from Stanford in 1970. He joined the Stanford Aero/Astro Department Faculty in 1971 and is currently an Emeritus Professor. Recent focus of research is centered around applications of GPS: applications of the FAA's WAAS for enhanced pilot displays, the use of WAAS and new displays to enable closer spacing on parallel runways, and the use of WAAS for flight inspection for conventional navigation aids. He has co-authored two text books in control systems design.

ABSTRACT

Maintaining the accuracy of an Instrument Landing System (ILS) is very important because it is the primary landing guidance system during bad weather in the U.S. Therefore, the FAA periodically checks the accuracy of an ILS and calibrates any deviation, a procedure called Flight Inspection (FI). In order to check the accuracy of an ILS, the FAA uses an Inertial-based Automated Flight Inspection System (AFIS). The Inertial-based AFIS is a self-contained system that has a navigation-grade inertial navigation system (INS), a barometric altimeter, a radar altimeter, GPS, and a TeleVision Positioning System (TVPS). Using these sensors and known runway coordinates, the Inertial-based AFIS is able to meet the ILS calibration accuracy requirement which is to measure the deviations of the ILS within 0.015 degree accuracy (as small as 30 cm in vertical). In fact, this accuracy requirement can also be achieved by using a commercial RTK DGPS system with much lesser cost than the Inertial-based AFIS. Those flight inspection systems that use RTK DGPS are called a DGPS-based AFIS. However, the relatively large set-up time of the DGPS-based AFIS is a serious limiting factor to the FAA because they have to check a large number of ILS's. Previously, from an effort to replace the Inertial-based AFIS to a lower cost system while maintaining or improving its efficiency and accuracy, WAAS-aided Flight Inspection System (WAAS-aided FIS) has been proposed [1]. This system uses a low grade INS, WAAS, a radar altimeter and a TeleVision Positioning System (TVPS). The advantages of this system are cheaper cost, better efficiency and better accuracy than the Inertial-based AFIS. The WAAS-aided FIS can be easily implemented in the Inertial-based AFIS due to the similarity of these two systems. However, the drawback of this system is the vulnerability to a possible accuracy degrade in rare events, for example a sharp ionospheric gradient and severe multipath, because only position outputs from the WAAS receiver can be used for the easy system realization from the Inertial-based AFIS.

In this paper, we introduce the "WAAS-based Flight Inspection System (WAAS-based FIS)" which overcomes the shortcomings of the other flight inspection systems. The WAAS-based FIS is a self-contained system, on the airplane, equipped with a single frequency WAAS receiver, a radar altimeter and a TeleVision Positioning System (TVPS). In this system, the estimated flight trajectory is the sum of an accuracy position fix over the runway threshold from the radar altimeter and the TVPS and the precise relative position with respect to the position fix. An advanced algorithm called "Time-Differenced Precise Relative Positioning Method" is used to provide the relative position, which uses time-differenced carrier phase measurements as ranging

sources and removes ionospheric delay effects by using code minus carrier phase measurements. This positioning scheme takes advantage of known runway coordinates and near-real time processing allowed in flight inspection. The WAAS-based FIS has been tested with flight test data taken in collaboration with the FAA, and the results confirm that the algorithm is able to produce position outputs that sufficiently meet the ILS calibration accuracy requirements. The advantages of the WAAS-based FIS are lower cost, better efficiency and better accuracy than the Inertial-based AFIS and more robustness than the WAAS-aided FIS.

INTRODUCTION

The Instrument Landing System (ILS) is the primary landing guidance in U.S. Therefore, the ILS must provide a proper guidance at all times and any installation. However, because of its sensitivity to surrounding environment, the accuracy of the ILS may significantly degrade if environmental changes occur near the ILS [2]. For this reason, the Federal Aviation Administraion (FAA) regularly checks and calibrates the ILS to maintain its accuracy.

The guidance of an ILS is checked through flight inspection. During a flight inspection, an aircraft approaches a runway following the ILS guidance. The flight path during approach is determined from a flight insepction system. This flight path is used to determine the errors in the desired ILS guidance. If there is a deviation in the ILS guidance, a calibration is required and done by ground crews.

The first instrument used for the ILS calibration was a theodolite, an instruments that measures horizontal and vertical angles [3]. Figure 1 shows the old fashioned ILS calibration procedure with a theodolite. This procedure required very skilled people and was time consuming. Then, an automatic light or laser tracker replaced the manual theodolites around 1970s~1980s [3]. Various trackers were used, but they all tracked light or laser from its source installed on the airplane. Flight paths were still estimated on the ground, and the overall ILS calibration procedure took a significant amount of time. During 1980s, the Inertial-based Automatic (or Automated) Flight Inspection System (AFIS) was developed [3, 4]. This system used a navigation grade INS (Inertial Navigation System) as a primary sensor with a barometeric altimeter, a radar altimeter, a camera system (TVPS), and a pilot event buttion. A kalman filter was used to estimate a flight trajectory by fusing the measurements from those sensors. This system is an automated self-contained system that made the ILS calibration procedure more efficient and conveinent. However, the drawbacks of the Inertial-based AFIS are high cost and degrading accuracy further from a runway. Also, an airplane needs to fly level over the whole runway to calibrate various biases in the INS. Irrespective of the drawbacks, this kind of AFIS has been contiuously evolved and is being used by the FAA and worldwide.

After precise positioning techniques using GPS were developed and commercialized around the 1990s [3], the techniques were adapted to a flight inspection system for the ILS calibration problem. This kind of FIS is called the Differential GPS-based Automatic Flight Inspection System (DGPS-based AFIS). This system usually provides a centimeter level of accuracy in real time without any drifts. However, it requires a time-consuming procedure in setting up a local reference station in each airport, which is the main drawback of the DGPS-based AFIS.

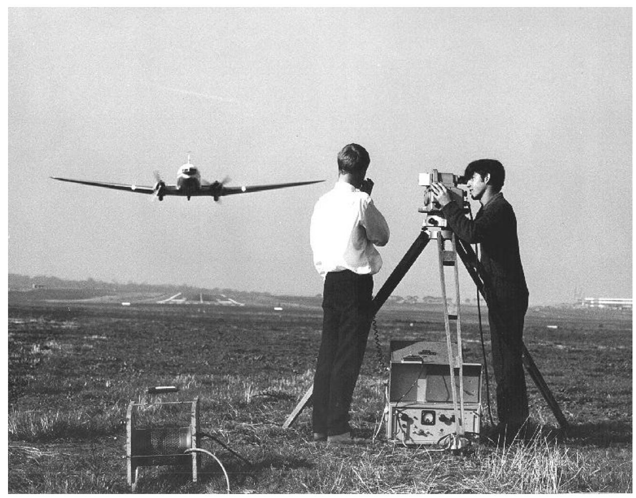

Figure 1: The two surveyors on the ground measure the aircraft's deviation from the desired flight path using a theodolite (courtesy of CAHS collection) [5]

Therefore, the current automated flight inspection systems are Inertial-based AFIS and DGPS-based AFIS whose characteristics are quite different in terms of cost, accuracy and efficiency. In the U.S., the FAA prefers to use the Inertial-based AFIS mainly due to its efficiency despite of the higher cost. To inspect numerous ILS's over the U.S., the efficiency is the most important factor. Previously, from an effort to replace the Inertial-based AFIS to a lower cost system, WAAS-aided Flight Inspection System (WAAS-aided FIS) was proposed [1]. This system uses a low grade INS, WAAS, a radar altimeter and a TeleVision Positioning System (TVPS). The advantages of this system are lower cost, better efficiency and better accuracy than the Inertial-based AFIS. Also, the WAAS-aided FIS can be easily implemented in the Inertial–based AFIS due to the similarity of these two systems. However, the drawback of this system is that it has the same vulnerability to a possible accuracy degrade in rare events that the WAAS has, for example a sharp ionospheric gradient and severe multipath, because it was constrained to only utilize position outputs from the WAAS receiver.

Figure 2: Modern computerized FIS (courtesy of NXT, Inc) [6]

From continuing efforts in replacing the Inertial-based AFIS to a lower system, we introduce the "WAAS-based Flight Inspection System (WAAS-based FIS)" in this paper. The WAAS-based FIS is a self-contained system equipped with a single frequency WAAS receiver, a radar altimeter and a TeleVision Positioning System (TVPS). A specialized positioning algorithm called "Time-Differenced Precise Relative Positioning (T-D PRP)" method is used for this system. The positioning algorithm uses the difference of carrier phase measurements at two epochs as ranging sources and utilizes WAAS correction messages. Taking advantage of near real-time positioning that is allowed in flight inspection, T-D PRP uses smoothed WAAS fast clock corrections and eliminates relative ionospheric delays at the two epochs. Not only does the WAAS-based FIS provide accurate position that meets flight inspection system accuracy requirements, its integrity is also affirmed from WAAS integrity messages and further safety checks. Those checks include an ionospheric delay compensation and the validation of a reference position from a radar altimeter and a TVPS. Overall, the WAAS-based FIS overcomes the shortcomings of the other FIS's and provides the optimized performance in the aspects of accuracy, cost, efficiency, and integrity.

This paper is organized as follows. First, the nature of the ILS calibration problem and its accuracy requirements are briefly introduced. Then, the details of the proposed WAAS-based FIS are discussed, including its system architecture, positioning algorithm, ionospheric delay compensation technique with a single frequency receiver, satellite exclusion tests, WAAS fast-clock correction filtering, and validation of a reference position from a radar altimeter and a TVPS. Thirdly, the test results from implementing the WAAS-based FIS with flight test data are presented. Lastly, the conclusions are provided.

ILS CALIBRATION PROBLEM AND FLIGHT INSPECTION SYSTEM ACCURACY REQUIREMENTS

An ILS consists of a glideslope, a localizer and marker beacons. A localizer and a glideslope provide horizontal and vertical guidance to a runway. Marker beacons alert a pilot of his/her approaching specific waypoints with an audible alert. Therefore, the guidance from a glideslope and a localizer is the main objective for the ILS calibration in flight inspection.

The ILS calibration problem is quite unique among other estimation problems. First, the aircraft's trajectory is allowed to be estimated in near real-time, i.e., within a few minutes of real time. Secondly, the surveyed runway threshold position can be used to estimate flight paths during approach and indeed is being used in the Inertial-based AFIS. Therefore, a flight inspection procedure using these features, as with the Inertial-based AFIS, can have two modes: approach mode and flight trajectory estimation and ILS calibration mode as illustrated in Figure 3. The duration of the approach mode is usually less than a few minutes. Therefore, only a short set of measurements is available. The accuracy required for flight inspection system is not rectilinear. Since the ILS is an angular guidance system, the accuracy requirements of a flight inspection system is also angular. The FAA uses the following guidelines. For CAT I ILS, an estimation error should be less than 0.05 deg from glideslope and localizer antennas but not less than 30cm in vertical and 60cm in cross-track. For CAT II/III ILS, an estimation error should be less than 0.015 deg from glideslope and localizer antennas but not less than 30cm in vertical and 60cm in cross-track. In other words, the accuracy requirements become looser as the distance from those antennas increases if XYZ Cartesian coordinates are used. The vertical flight inspection system accuracy requirements for ILS calibration are shown in Figure 4.

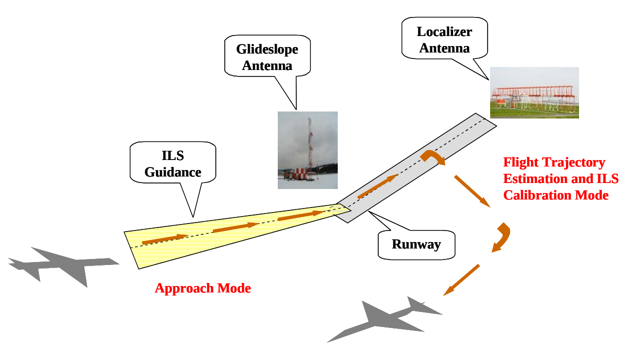

Figure 3 : Two Flight Inspection Modes in ILS Calibration

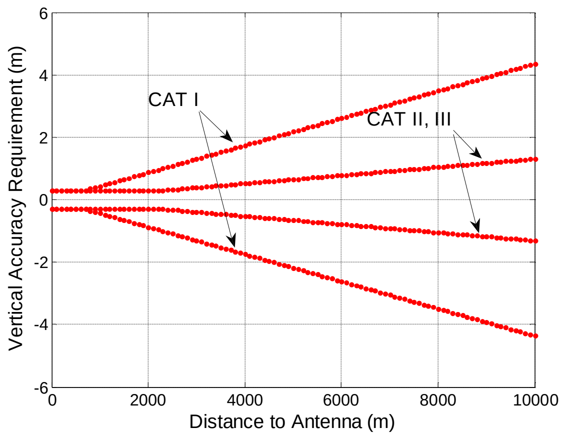

Figure 4: Vertical flight inspection system accuracy requirements for ILS calibration

WAAS-BASED FLIGHT INSPECTION SYSTEM

This section discusses the details of the WAAS-based Flight Inspection System (FIS). The overall architecture and its specific positioning algorithms are presented. Also, integrity features in this system are addressed.

a. Why Use WAAS for ILS Calibration?

WAAS position solutions and integrity can't be directly used for the ILS calibration problem because it is lacking in accuracy. WAAS 95% accuracy is better than 0.935 meters in horizontal and 1.289 meters in vertical [7], which does not meet the ILS calibration accuracy requirements. The WAAS integrity provides real-time error bounds, but the bounds are in the level of tens of meters and not useful for the ILS calibration problem.

However, the WAAS broadcast messages still have a lot to offer. First, the WAAS broadcasts accurate correction messages for satellite clock-ephemeris errors and ionospheric delay correction errors. Secondly, the WAAS issues a flag when satellite anomalies and severe ionospheric disturbances occur. These features play a very important role in helping the WAAS-based FIS have sound position solutions and firm integrity.

b. System Architecture

The WAAS-based FIS is a system that has a single frequency WAAS receiver, a radar altimeter, a TVPS (TeleVision Positioning System) and a computer. The 95% accuracies of a radar altimeter and a TVPS used in the current Inertial-based FIS are better than 15cm [8, 9]. The same kinds of radar altimeter and TVPS are assumed for the WAAS-based FIS. This integrated system is optimally designed for the ILS calibration problem in terms of accuracy, cost, efficiency and integrity.

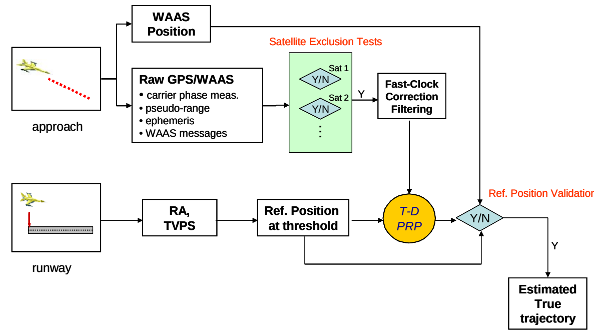

Figure 5 : System architecture of WAAS-Based FIS

Figure 5 illustrates the overall algorithm of the WAAS-based FIS. During approach, WAAS position and raw GPS/WAAS measurements are collected. The GPS/WAAS measurements include ephemeris, L1 code and carrier phase measurements, and WAAS messages. Over the threshold of a runway, the radar altimeter measures the vertical distance of the airplane from the runway threshold and the TVPS measures the cross-track deviation of the airplane from the centerline of the runway. Since the position of the threshold is accurately surveyed, the radar altimeter and the TVPS provide an accurate instant position of the airplane over the threshold. A specialized positioning algorithm, Time-Differenced Precise Relative Positioning (T-D PRP) method, uses this reference position and the raw measurements to compute precise relative positions. The estimated flight trajectory during approach is obtained by adding the relative positions to the reference position. The detailed algorithm of the T-D PRP will be discussed in the next subsection. There are two integrity features for the soundness of the estimated flight trajectory: satellite exclusion tests and validation of the reference position from the radar altimeter and the TVPS. Satellite exclusion tests are implemented to discard a satellite that should not be used in T-D PRP for various reasons. The integrity of a reference position from a radar altimeter and a TVPS is checked using both WAAS position during approach and the precise relative position from the T-D PRP. Even though this validation test is limited to the level of WAAS accuracy, it is useful when a radar altimeter or a TVPS introduces an abnormally large error. The two integrity features will be further discussed later in this section

c. Time-Differenced Precise Relative Positioning

The difference of carrier phase measurements at two epochs has been proposed as a source for velocity or relative position, for example [10, 11]. The formulation used in [10] and [11] is essentially same, but [10] used it for relative position estimation and [11] used it for precise velocity estimation. The time-differenced precise relative positioning (T-D PRP) proposed in this paper uses the same formulation and also computes relative positions with a single frequency receiver. However, the main difference from the previous approaches is that the ionospheric delay gradient at two epochs is estimated and removed using the combination of L1 code and carrier phase measurements in near real time. The ionospheric delay gradient estimation with a single frequency receiver was recently introduced in [12] and will be briefly discussed in the next subsection.

Carrier phase measurements from a GPS satellite have the following expression.

$$\Phi = r + c[\delta t_u - \delta t_s] - I + T + N + \varepsilon \quad (1)$$

where r is the true range between a receiver and a satellite, c is the speed of light, and δt_u and δt_s are receiver and satellite clock errors, respectively. I is an ionospheric delay in L1 frequency and T is a tropospheric delay. N is an integer ambiguity. ε includes multipath, thermal noises, and modeling errors in carrier phase measurements.

Assuming that there is no cycle-slip, a single difference of carrier phase measurements from a satellite k at two epochs, t and 0, is as follows.

$$\Phi_t^k - \Phi_0^k = r_t^k - r_0^k + c\Delta t_u - c\Delta t_s^k - \Delta I_t^k + \Delta T_t^k + \Delta\varepsilon_t^k \quad (2)$$

where $\Delta(\cdot)$ is the difference of the same variable at the two epochs.

Now, applying WAAS satellite clock-ephemeris error corrections and tropospheric error correction to (2) and linearizing it with respect to a reference position, (2) becomes with a short base line assumption

$$\begin{aligned} y_{t,0}^k &= r_t^k - r_0^k - (\hat{r}_{R,t}^k - \hat{r}_{R,0}^k) + c\Delta t_u - \Delta I_t^k + \Delta\tilde{\varepsilon}_t^k \\ &= -1_t^k \cdot \delta\overline{x}_{t,0} + c\Delta t_u + b_{\text{Ref},t}^k - \Delta I_t^k + \Delta\tilde{\varepsilon}_t^k \end{aligned} \quad (3)$$

where $\hat{r}_R^k$ is the computed distance between the satellite k and a reference position using the broadcast ephemeris. 1_t^k is a line of sight vector to the satellite k at time t. $\delta\overline{x}_{t,0}$ is a relative position of a receiver from the position at time 0. $b_{\text{Ref},t}$ is an error caused from the imperfect knowledge of reference position at time t. $\Delta\tilde{\varepsilon}_t^k$ includes residual correction errors and higher order modeling errors due to linearization in addition to $\Delta\varepsilon_t^k$.

It is helpful to appreciate the error characteristics of (3) to see why this formulation is used in the WAAS-based FIS. Since $c\Delta t_u$ is common to the all satellites, it should be easily estimated. Therefore, the error sources in (3) are $b_{\text{Ref},t}$, ΔI, and $\Delta\tilde{\varepsilon}$.

Now, let us assume that we know satellite locations perfectly to see the sole effects of reference position errors. When the exact reference position is known, $b_{\text{Ref},t}$ is zero. However, when the reference position has some errors, the computed distance between the satellite k and a reference position has the following expression.

$$\hat{r}_{R,t}^k = r_{R,t}^k + 1_t^k \cdot \delta\overline{x}_{\text{bias}} \quad (4)$$

where $\delta\overline{x}_{\text{bias}}$ is a reference position error vector from a true position the erroneous reference position. Then,

$$\begin{aligned} r_t^k - \hat{r}_{R,t}^k &\approx -1_t^k \cdot \delta\overline{x}_{t,0} - 1_t^k \cdot \delta\overline{x}_{\text{bias}} \\ -r_0^k + \hat{r}_{R,0}^k &\approx 1_0^k \cdot \delta\overline{x}_{\text{bias}} \end{aligned} \quad (5)$$

Therefore, $b_{\text{Ref},t}^k$ is

$$b_{\text{Ref},t}^k \approx -1_t^k \cdot \delta\overline{x}_{\text{bias}} + 1_0^k \cdot \delta\overline{x}_{\text{bias}} \quad (6)$$

From (6), we can see that $b_{\text{Ref},t}^k$ is small when t is near to zero and increases as t increases.

Next, ΔI is estimated and removed by using the difference of L1 code and carrier phase measurements, assuming that ΔI linearly behaves during approach. More details of the estimation of ΔI will be discussed in the next subsection.

$\Delta\tilde{\varepsilon}_t^k$ includes tropospheric delay correction residuals, satellite clock-ephemeris correction residuals, multipath, modeling errors, thermal noise and so on. $\Delta\tilde{\varepsilon}_t^k$ is also very small when t is near to zero and increases as t increases because the residual correction errors are highly correlated [13, 14]. Fortunately, multipath and other receiver related noise are small (~1 or 2cm) enough for our application that they are not of our concern.

Overall, the error characteristic of the single difference of the carrier measurements is that the error is very small when t is near to zero and grows over time. This error characteristic is well suited for the ILS calibration problem as long as the errors are kept low enough not to violate the ILS calibration accuracy requirement. Once ΔI is removed, the level of error that grows over time is insignificant for the ILS calibration problem.

A set of linear equation can be formed as follows.

$$\underbrace{\begin{bmatrix} y_{t,0}^1 \\ y_{t,0}^2 \\ \vdots \\ y_{t,0}^n \end{bmatrix}}_{Y} = \underbrace{\begin{bmatrix} -1_t^1 & 1 \\ -1_t^2 & 1 \\ \vdots & \\ -1_t^k & 1 \end{bmatrix}}_{G} \underbrace{\begin{bmatrix} \delta \bar{x}_{t,0} \\ C\Delta t_u \end{bmatrix}}_{X} + \underbrace{\begin{bmatrix} \hat{\varepsilon}_t^1 \\ \hat{\varepsilon}_t^2 \\ \vdots \\ \hat{\varepsilon}_t^k \end{bmatrix}}_{\hat{\varepsilon}}$$

$$Y = GX + \hat{\varepsilon} \tag{7}$$

where $\hat{\varepsilon}$ includes $b_{\mathrm{Ref},t}$, $\Delta\tilde{\varepsilon}_t$, and residual errors from the compensation of ΔI.

Then, the relative position from T-D PRP with respect to the reference position is computed using weighted least squares as follows

$$X = (G^T W^{-1} G)^{-1} G^T W^{-1} Y \tag{8}$$

where W is a weighting matrix. It is difficult to find W because some of the errors in Y are highly correlated over time. However, since the overall errors have dependency on a satellite elevation angle, a reasonable choice for its elements would be as a function of the satellite elevation angle.

d. Ionospheric Delay Gradient Estimation using Linear Regression with a Single Frequency Receiver

This subsection gives a brief review of ionospheric delay gradient estimation with a single frequency receiver introduced in [12]. The estimated ionospheric delay gradient is used to make a correction for the differential ionospheric delays between a reference position and any points during approach, which makes the WAAS-based FIS robust to various ionospheric effects with a single frequency receiver.

The basic measurements from a GPS satellite are code and carrier phase measurements. The carrier phase measurement is already expressed in (1). The code phase measurements, ρ, can be written as

$$\rho = r + c[\delta t_u - \delta t_s] + I + T + M \tag{9}$$

where M includes multipath, thermal noises, and modeling errors in the code phase measurement.

The code minus carrier phase measurement at time t is

$$\rho_t - \Phi_t = 2I_t - N + M_t - \varepsilon_t \tag{10}$$

This difference includes ionospheric delays multiplied by 2, an integer ambiguity and noise in code and carrier phase measurements. Our interest, here, is to estimate a slant ionospheric delay rate. It should be noted that the ionospheric delays slowly change with respect to time during nominal ionospheric days. Therefore, the rate can be seen as a constant during a short time window (tens of minutes). Assuming a constant ionospheric delay rate, equation (10) can be rewritten as

$$\begin{aligned} \rho_t - \Phi_t &= \beta_0 + 2t \cdot \beta_1 + M_t - \varepsilon_t \\ &\approx \beta_0 + 2t \cdot \beta_1 + M_t \end{aligned} \tag{11}$$

In equation (11), ε_t is ignored because it is much smaller than M_t.

Expressing the time series of equation (11) in a matrix form yields

$$\underbrace{\begin{bmatrix} \rho_{t_0} - \Phi_{t_0} \\ \rho_{t_1} - \Phi_{t_1} \\ \vdots \\ \rho_{t_n} - \Phi_{t_n} \end{bmatrix}}_{\tilde{Y}} = \underbrace{\begin{bmatrix} 1 & 2 \cdot t_0 \\ 1 & 2 \cdot t_1 \\ & \vdots \\ 1 & 2 \cdot t_n \end{bmatrix}}_{R} \underbrace{\begin{bmatrix} \beta_0 \\ \beta_1 \end{bmatrix}}_{\beta} + \underbrace{\begin{bmatrix} M_{t_0} \\ M_{t_1} \\ \vdots \\ M_{t_n} \end{bmatrix}}_{M}$$

$$\tilde{Y} = R\beta + M \tag{12}$$

Now, the problem becomes to find β in the presence of M. If M is white nose, the ordinary least-squares (OLS) is the best estimator. Fortunately, airborne multipath is very close to white noise [12]. Therefore,

$$\hat{\beta}_{OLS} = (R^T R)^{-1} R^T \tilde{Y} \tag{13}$$

Once we have the estimated ionospheric delay gradient, $\hat{\beta}_1$, the differential ionospheric delay correction between a reference position and any points during approach is simply

$$\Delta \hat{I}_{t,0} = t \square \hat{\beta}_1 \tag{14}$$

It is interesting to see how much the estimated ionospheric delay gradient is useful even during ionospheric nominal days. Figure 6 compares relative positions from implementing the T-D PRP with and without compensating for the differential ionospheric delays using static experimental receiver data. The error growth was significantly reduced when the differential ionospheric delays were compensated.

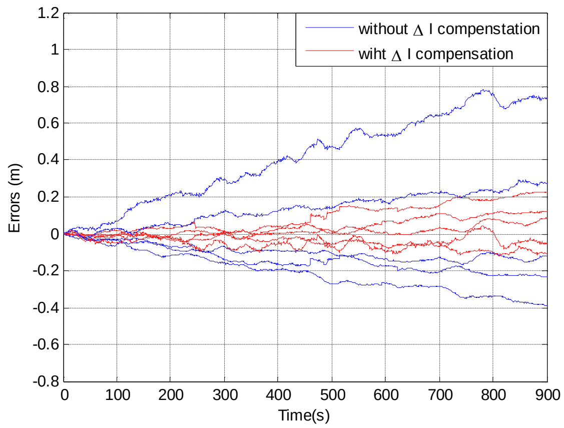

Figure 6: Example of the effectiveness in applying $\Delta\hat{I}$ based on the measurement taken on 09/05/2005

e. Satellite Exclusion Tests

To ensure safe position solutions from the T-D PRP, it is necessary to detect any threats and exclude them. This section discusses how to choose the right set of satellites for the T-D PRP using WAAS integrity messages and other internal sanity check procedures.

Figure 7 shows a chart of the items that should be checked before including a satellite in the T-D PRP. The first safety check is to see if there are any GPS/WAAS UNHEALTHY or WAAS UNMONITORED designations. If these messages are delivered from GPS/WAAS for a particular satellite, that satellite will be excluded. Similarly, a satellite having UDREI greater than or equal to 12 will be excluded as well because that satellite may have some problem and can't be used for WAAS-based precision approach [15].

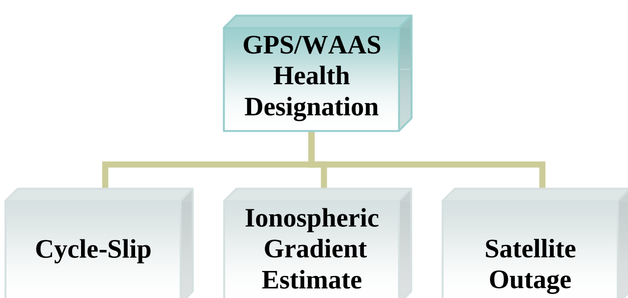

Figure 7: Chart of items for satellite exclusion criteria.

Any satellite experiencing a cycle-slip during approach is also excluded because the T-D PRP must use continuously accumulated carrier phase measurements. In addition, the goodness of fit for the estimation of ionospheric delay gradient must be examined. Any ionospheric delay gradients showing a severe nonlinear behavior can be detected by analyzing the residuals after fitting a first order linear model on code minus carrier phase measurements. Chi-square tests will are a good indicator for goodness of fit [16]. Lastly, it is best to use the same set of satellites during the entire approach. A different set of satellites may introduce a sudden jump in relative positions, which is very undesirable for our application.

f. Fast-Clock Correction Filtering

Interestingly, WAAS positions typically have a 12 seconds periodic noise [1]. The main source of this periodic noise is fast-clock correction messages and range rate corrections (RRC). The broadcast fast clock correction has a 0.125 meters resolution and often shows a 12 seconds period pattern. The fast clock correction message must be filtered or smoothed to result in a fine resolution in position solutions. Fortunately, the RRC can be easily turned off by setting it to zero in the receiver, which is permitted since SA (Selective Availability) is turned off.

Figure 8 shows a typical example of the broadcast fast clock corrections and smoothed fast clock corrections. The smoothing process takes place after receiving all the messages during approach. Since the message has 12 seconds periodic pattern for considerable amount of time, a non-causal moving average filter having 12 seconds or a multiple of 12 seconds length will remove the periodic pattern.

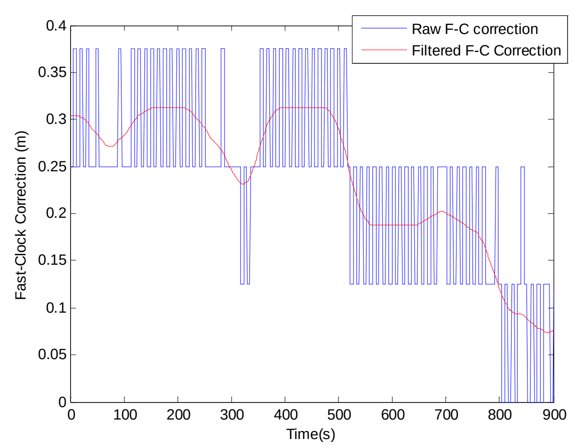

Figure 8: Example of fast-clock correction filtering

g. Validation of a Reference Position from Radar Altimeter and TVPS

A radar altimeter and a TVPS provide a reference position over a threshold. Since the estimated flight path is the sum of the reference position and the relative position from the T-D PRP, the accurate measurements from those sensors are extremely important. This subsection discusses how to validate the reference position using WAAS position.

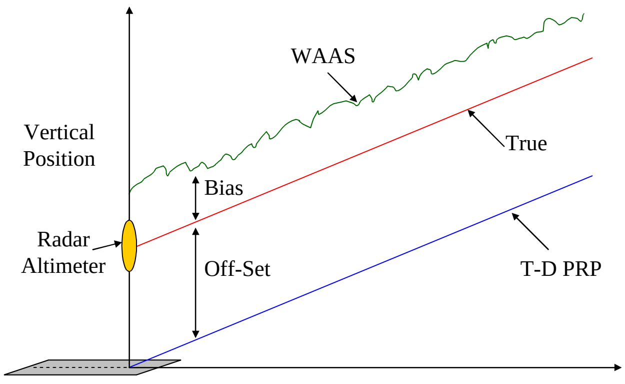

Figure 9: Schematics of the characteristics of three position measurements (R.A, WAAS, TD-PRP) with true position

Figure 9 depicts how a true flight trajectory is related with WAAS position and the relative position from the T-D PRP in vertical. Basically, WAAS position has a constant bias and noise on top of the true position during approach [1]. On the other hand, the position from the T-D PRP is precise but has an off-set to the true position. In mathematical expression, these positions can be described as follows.

$$\begin{aligned} &\text{WAAS} = \text{True} + \text{Bias} + \text{Noise} \\ &\text{T-D PRP} = \text{True} - \text{Off-Set} \end{aligned} \qquad (15)$$

Taking the average of the difference of the WAAS position and the T-D PRP position during approach yields the following expression.

$$\begin{aligned} AVG_{(\text{WAAS}-\text{T-D PRP})} &= \frac{1}{n}\sum_{t=0}^{n}(\text{WAAS}-\text{T-D PRP})_t \\ &\approx \text{Bias} + \text{Off-Set} \end{aligned} \qquad (16)$$

In (16), the noise in WAAS position are averaged out to near zero.

Now, an instantaneous measurement of a radar altimeter over the threshold has an off-set and a small error as follows.

$$\text{Radar Altimeter} = \text{True}_{\text{thr}} + \text{Error} \qquad (17)$$

Then, the difference of measurements of a radar altimeter and T-D PRP over the threshold is

$$\begin{aligned} \Delta_{(\text{RA}-\text{T-D PRP}_{\text{thr}})} &= \text{Radar Altimter} - \text{T-D PRP}_{\text{thr}} \\ &= \text{Error} + \text{Off-set} \end{aligned} \qquad (18)$$

Then, if we subtract (18) from (16), the remaining term is approximately the sum of the WAAS bias and the small error from the radar altimeter as follows.

$$AVG_{(\text{WAAS}-\text{T-D PRP})} - \Delta_{(\text{RA}-\text{T-D PRP}_{\text{thr}})} \approx \text{Bias} - \text{Error} \quad (19)$$

The message from (19) is that once we know the statistical distributions of the WAAS bias and the errors from a radar altimeter, which is already presented in the previous sections, we can also form a distribution of (19) . Using this distribution, it is possible to check where the value of (19) stands on the distribution for each approach. If the value is beyond a threshold, for example 95% with two sided Gaussian distribution, a flag is raised to indicate a possible corruption in the radar altimeter measurement. A similar procedure can be used in horizontal with a TVPS. Considering the 95% accuracies of the WAAS, a radar altimeter, and a TVPS, the thresholds (2σ) are 1.11 meters in horizontal and 1.3234 meters in vertical respectively.

FLIGHT TEST RESULTS

For the validation of the WAAS-based FIS, the algorithm was tested with flight test data taken during Oct 30~31, 2006 in collaboration with the FAA AVN at Oklahoma City. During the flight test, DGPS positions from a RTK system were also collected in addition to raw GPS/WAAS data. Therefore, the DGPS positions were used as a truth source for the validation of the WAAS-based FIS. A Radar altimeter and a TVPS were not used because there were some hardware difficulties during the tests. So, the reference positions were provided from the DGPS and the validation of the reference positions was not implemented. Figure 10 shows an example of flight paths during the flight tests in ENU coordinates. The total number of approaches used in this test is 23.

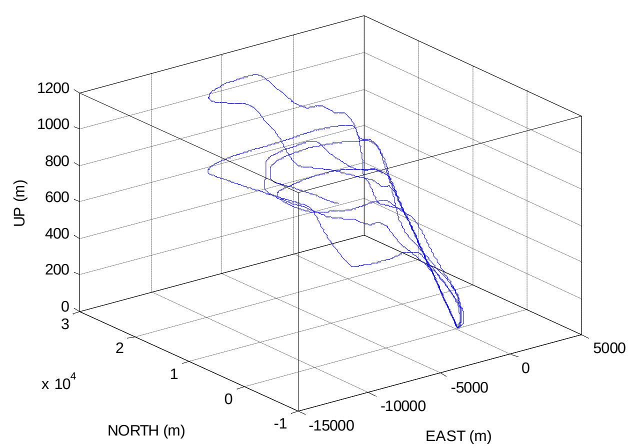

Figure 10: Some of the flight trajectories in flight tests taken during Oct 30~31, 2006 in the FAA at Oklahoma City

T-D PRP Tests

Figure 11 and Figure 12 shows the horizontal and vertical errors from implementing the T-D PRP with a reference position given from a DGPS position. The two red lines are flight inspection system accuracy requirements for CAT I and CAT II, III ILS calibration.

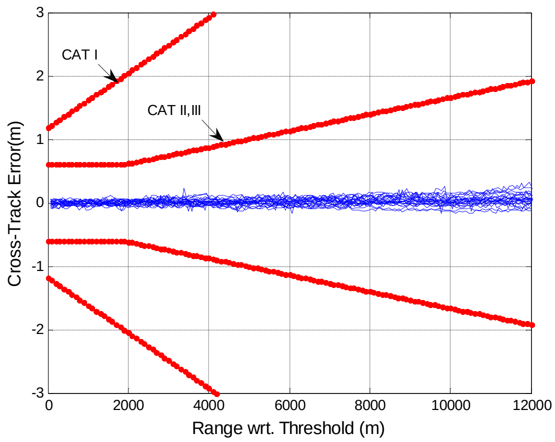

Figure 11: Cross-track errors in meters of 23 approaches from WAAS-based FIS (without TVPS errors)

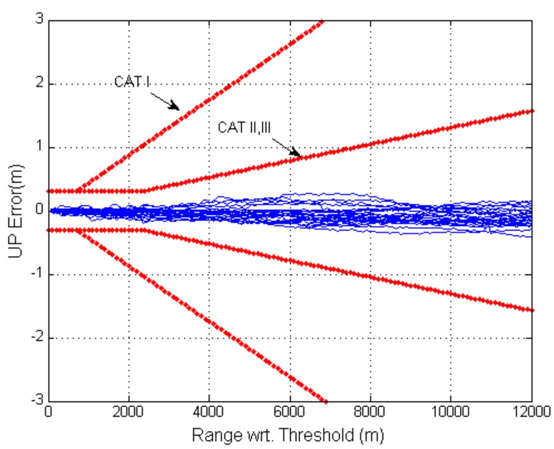

Figure 12: Vertical error in meters of 23 approaches from WAAS-based FIS (without RA errors)

Figure 11 and Figure 12 do not represent the total errors of WAAS-based FIS tests because the reference position errors are not included. However, these results clearly show the error characteristics of the T-D PRP, which slowly increase over time. Based on that, it is possible to measure the performance of WAAS-based FIS using 95% accuracies of a radar altimeter and a TVPS.

WAAS-based FIS Performance

To see the accuracy of the WAAS-based FIS, we should consider the total errors caused by both the T-D PRP and the reference position error. Considering the errors from the T-D PRP and the accuracy requirements, the most critical regions are around 2200 meters and 2000 meters from the threshold in vertical and horizontal respectively. The error distribution of the T-D PRP in the critical regions is important because the total errors, sum of the errors from T-D PRP and reference position errors, most likely violate the flight inspection system accuracy requirements for CAT II, III ILS calibration. Table 1 summarized the statistics of the errors from the T-D PRP at the critical regions.

	Up (m)	Cross-Track (m)
Mean	-0.035	0.002
Std	0.051	0.041
RMS	0.061	0.041

Table 1: Statistics of the T-D PRP Errors at Critical Regions

Treating the T-D PRP errors and reference position errors as independent random variables with zero mean, which is not exactly true but practically good enough, the distributions of the total errors can be easily calculated. Since the accuracies (95%) of a radar altimeter and a TVPS are about 15cm, the total errors at the critical regions have 9.06cm standard deviation in vertical and 8.55cm standard deviation in cross-track. Therefore, the 95% accuracy of the WAAS-based FIS is 18.14cm meters in vertical and 17.09cm in cross-track at the critical regions. Therefore, the WAAS-based FIS sufficiently meets the flight inspection system accuracy requirements up to CAT II, III ILS calibration whose limits are about 30cm in vertical and 60 cm in cross-track.

CONCLUSION

In this paper, the WAAS-based FIS is introduced. Its system architecture, positioning algorithm and integrity features are thoroughly discussed. For the validation of the WAAS-based FIS algorithm, this system was tested with flight test data taken during Oct 30~31, 2007 at Oklahoma City. The results were shown to meet the required accuracy for flight inspection of CAT I,II, and III ILS's.

Overall, the WAAS-based FIS provides more optimized performance than the other flight inspection systems in terms of accuracy, cost, efficiency and integrity. Its accuracy is between the Inertial-based AFIS and the DGPS-based AFIS, and its cost is significantly lower than the two AFIS's. The efficiency of the WAAS-based FIS outperforms the two AFIS' because it does not need a reference station on the ground nor does it require the FI aircraft to fly level over the whole runway. The WAAS-based FIS also provides secure redundant integrity features using the WAAS messages and internal safety checks. It should be noted, however, that the scheme does require that modification be made to a certified WAAS receiver.

ACKNOWLEDGMENTS

The authors gratefully acknowledge the support of FAA flight inspection division (AVN)

REFERENCES

[1] E. Kim, T. Walter, and J.D. Powell, "*A Development of WAAS-Aided Flight Inspection System*", In Proc. IEEE/ION PLANS 2006, San Diego, Apr 24-27, 2006
[2] M. Kayton and F. Walter, *Avionics Navigation Systems.* New York: John Wiley and Sons, 1997
[3] *Flight Inspection History,* International Committee for Airspace Standards and Calibration (ICASC), Available : http://avnwww.jccbi.gov/icasc/fi_history.html
[4] M.S. Bruno and M.F. Cecelia, "*The Design, Simulation, and Implementation of an Accurate Positioning System For Automatic Flight Inspection System*", In Proc. IEEE PLANS 1990, Las Vegas, Mar 20-23, 1990
[5] ILS Calibration by DC3, Available: http://www.airwaysmuseum.com/DC3%20ILS%20calibration.htm
[6] JCAB Gulfstream IV Flight Inspection System, Available: www.nxt-afis.com/products_home.htm
[7] *Wide-Area Augmentation System Performance Analysis Report*, FAA William J. Hughes Technical Center, Atlantic City, NJ (updated reports issued every quarter). Available: http://www.nstb.tc.faa.gov/ArchiveList.html
[8] U. Peled, "*Radar Altimeter Evaluation-Refined Runway Data*", internal report, Stanford, California, May 28, 2005
[9] Television Positioning System, NXT. Flight Inspection Systems, Available: http://www.nxt-afis.com/television_positioning_system.html
[10] E.M. Somerville an J.F. Raquet, "*Self-Differential GPS-What are the Limits?*", In Proc. ION NTM 2006, Monterey, Jan 19-20, 2006
[11] F.V. Graas and A. Soloviev, *"Precise Velocity Estimation Using a Stand-Alone GPS Receiver"*, In Proc. ION NTM 2003, Anaheim, Jan 22-24, 2004
[12] E. Kim, T. Walter, and J.D. Powell, "*Adaptive Carrier Smoothing using Code and Carrier Divergence*", In Proc. ION NTM 2007, San Diego, Jan 22-24, 2007
[13] T. Walter, A. Hansen, and P. Enge, "*Validation of the WAAS MOPS Integrity Equation*", In Proc. ION Annual Meeting 1999, Cambridge, June 28-30, 1999
[14] H.E. Ibrahim and A. El-Rabbany, "*Stochastic Modeling of Residual Tropospheric Delay*", In Proc. ION NTM 2007, San Diego, Jan 22-24, 2007
[15] *Minimum Operational Performance Standards for Global Positioning System/Wide Area Augmentation System Airborne Equipment.* Washington, D.C, RTCA SC-159, WG-2, DO-229C, 28 Nov, 2001.
[16] Yaakov Bar-Shalom et al., *Estimation with Application to Tracking and Navigation* ,New York, Wiely-InterScience, 2001